

## A STUDY ON CHRONIC MULTIPLE OVERLAPPED STENOSED ARTERIES USING BINGHAM PLASTIC FLUID MODEL OF BLOOD FLOW

*K. Bitrus, P.I. Ibenu and I. A. Adeniyi*

Department of Mathematical Sciences, Federal University Lokoja, P.M.B 1154,  
Lokoja, Kogi State, Nigeria

### *Abstract*

---

*We present a study on Bingham characteristics of blood flow through an arterial segment with multiple overlapped stenosis with no or negligible stenosis distance. The case is considered to be chronic, as almost every point on the wall is affected. Empirical Analysis was carried out to illustrate the effect any significant change in the stenosis shape, stenosis height and the parameter  $\gamma$  has on the resistance to flow. The results are presented graphically. It was found that a small increase in the stenosis height brings about high resistance to the blood flow as it narrows the flow region. Similarly, an increase in the stenosis shape parameter causes an increase in shear stress with the magnitude of increase being greater for small values of  $S$ . In addition, as the stenosis distance tends to zero the magnitude of shear stress on the wall also increases tremendously.*

---

**Keywords:** Bingham plastic model, Chronic, Stenosed artery, flow resistance, shape parameter, wall shear stress

### **I. Introduction**

Arteries, veins and capillaries are responsible for the transportation of blood through the human body. In some situations, unusual deposition of cholesterols, fats and plaques in the inner lining of arteries and veins over a long period of time causes these passages to be tightened and may result in the development of some cardiovascular diseases mainly atherosclerosis which is medically termed as stenosis. As a result, numerous studies on the characteristics of blood flow in arteries or veins having stenosis have been carried out in order to provide better understanding of atherosclerosis, thereby improving medical procedures associated with the disease.

The effect of magnetic field on *poiseuille* flow of Bingham plastic fluid model, for blood with velocity slip and non-slip was investigated by [1], and it was shown that the flow of blood can be controlled by applying magnetic field; A mathematical model was further developed for such a problem. It was also revealed that when the Hartmann number increases, the fluid velocity is greatly affected. In [1,2], a mathematical model for the study of multiple stenosis was formulated and solved to see the effect of multiple stenosis on flow characteristics of streaming blood through the atherosclerotic artery. In the studies, the Bingham plastic fluid model of blood was utilized to represent the non-Newtonian character of blood. It was observed that the stenotic and physical parameter have considerable effect on the blood flow behavior. Furthermore, in [2], some important observations with significant medical implications were made concerning the medical effect on the flow of blood in a stenosed artery. The resistance to flow-ratio for yield stress was determined in [3] and it was observed that it moves nearer to unity as the yield stress increases and flux decreases, the study also revealed that a variation in viscosity had significant effect in the resistance to flow-ratio. The degree of these changes was found to be maximum for yield stress and slightest for flux.

The study of axial symmetric, laminar, steady and one-dimensional flow of blood through narrow stenotic vessel was considered in [4] taking blood as Bingham plastic fluid. The analytical results showed that resistance to flow and the wall shear stress increases with the size of the stenoses but these increments is however small due to the non-Newtonian nature of blood. A mathematical model was also developed in [2,5] to study the effect of multiple stenosis on flow characteristics of streaming blood, through atherosclerotic artery using the Bingham fluid model.

Current literature indicates that focus has been directed at studies on blood flow through a stenosed arteries with multiple stenosis while taking into account the distance between the stenosis but not considering the fact that as the disease becomes chronic, the stenosis keep on multiplying leading to negligible distance between successive stenosis and causing a high resistance to blood flow. This is the kind of situation that may lead to stroke, ischemia, heart attack and many cardiovascular diseases. Cardiac ischemia is caused due to the constriction responsible for insufficient flow of blood through the coronary arteries into the heart [5].

---

Correspondence Author: Bitrus K., Email: kefas.bitrus@fulokoja.edu.ng, Tel: +2348063100817

*Transactions of the Nigerian Association of Mathematical Physics Volume 10, (July and Nov., 2019), 157 –164*

The flow of blood through narrow arteries with bell/belt-shaped stenosis, treating blood as casson fluid, was investigated in [6] and it was observed that the resistance to flow and skin friction increases with the increase in maximum depth of the stenosis. In addition, the effect of an overlapping stenosis on blood flow characteristics in a narrow artery was investigated in [6,7]. The steady flow of blood to act as a non-Newtonian fluid was analyzed in [8] and it was reported that the shear stress is proportional to the shear rate and that for Newtonian and non-Newtonian fluid, flow rate decreases with an increase in the dynamic viscosity of the blood.

This study/work considers the chronic case of the disease, that is, when the stenosis distance is negligible. This might be as a result of many/multiple stenosis in the artery or vein. The rest of the paper is organized as follows: In the next Section, the problem is introduced and formulated. We present boundary conditions in the Section that follows. In the fourth section, numerical computations and graphical representations are presented. Concluding remarks are given in the last section.

**II. Formulation of the problem**

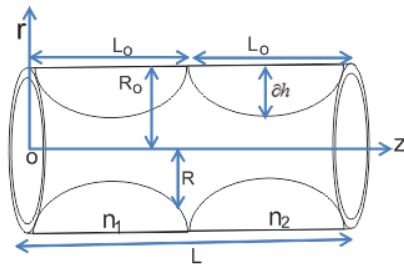


**Figure 1.** Geometrical representation of a chronically stenosed artery

Consider the flow of blood in an artery with overlapped stenosis; where the stenosis is symmetrical to the axis of flow but non symmetrical with respect to the radial coordinate of the artery. We assume there is no distance between the stenosis, thus, the position ( $d$ ) of the stenosis usually considered in the previous works is taken to be zero and the resistance to the flow is expected to be very high. The mathematical geometry of the stenosed artery with stenosis position ( $d$ ) is given as follows:

$$\frac{R}{R_0} = \begin{cases} 1 - \varepsilon \left[ L_0^{s-1} \{ \gamma z - nd - (n-1)L_0 \} - \{ \gamma z - nd - (n-1)L_0 \}^s \right], & n(d+L_0) - L_0 \leq \gamma z \leq n(d+L_0) \\ 1, & \text{otherwise} \end{cases} \quad (1)$$

with  $d$  as the position of the stenosis

Now on rewriting (1) and assuming the stenosis are overlapped with negligible between them, thus equation (1) is reduced to (2) as shown below.

$$\frac{R}{R_0} = \begin{cases} 1 - \varepsilon \left[ L_0^{s-1} \{ \gamma z - (n-1)L_0 \} - \{ \gamma z - (n-1)L_0 \}^s \right], & (n-1)L_0 \leq \gamma z \leq nL_0 \\ 1, & \text{otherwise} \end{cases} \quad (2)$$

where

$R$  : is the tube radius with stenosis

$R_0$  : is the tube radius without stenosis

$L_0$  : is the stenosis length

$s$  : Stenosis shape parameter and  $s \geq 2$

$r$  : A positive constant  $\geq 1$

$$\varepsilon = \frac{\delta h}{R_0} \frac{s}{L_0^s (s-1)}, \quad (3)$$

Such that the maximum height of the stenosis at

$$z = \frac{(n-1)L_0 + L_0 / s^{1/s-1}}{\gamma} \quad (4)$$

$$\beta = f(\tau) = -\frac{dv}{dr} = \begin{cases} \tau - \tau_0, & \tau \geq \tau_0 \\ \mu, & \tau \leq \tau_0 \\ 0, & \tau \leq \tau_0 \end{cases} \quad (5)$$

The flux  $Q_z$  through the artery is expressed mathematically as follows:

$$Q_z = \int_0^{2\pi} \int_0^R (rv(r)dv) d\theta \quad (6)$$

$$Q_z = 2\pi \int_0^R rv(r)dv \quad (7)$$

**III. Boundary Conditions**

The flow is considered to be axial and has no slip condition thus

$$\text{at } r = R, v = 0 \tag{8}$$

$\tau$  is finite at  $r = 0$ . At the boundary, that is, when  $r = R$ , the expression for shear stress in terms of the pressure gradient  $p$  is given as:

$$\tau = -\frac{r}{2} \frac{dp}{dz} \text{ and } \tau_R = -\frac{R}{2} \frac{dp}{dz} \Rightarrow \frac{\tau}{\tau_R} = \frac{r}{R} \tag{9}$$

Integrating (7) and using the boundary conditions in (8) yields (10)

$$Q_z = \pi \int_0^R r^2 \left( -\frac{dv}{dr} \right) dr \tag{10}$$

By careful consideration of (5) we can freely rewrite (10) as

$$Q_z = \pi \int_0^R r^2 f(\tau) dr \tag{11}$$

With the help of (9) we have

$$Q_z = \pi \frac{R^3}{\tau_R^3} \int_0^{\tau_R} \tau^2 f(\tau) d\tau = \pi \frac{R^3}{\tau_R^3} \int_0^{\tau_R} \tau^2 \frac{\tau - \tau_o}{\mu} d\tau \tag{12}$$

$$Q_z = \frac{\pi R^3}{\mu \tau_R^3} \left[ \frac{\tau_R^4}{4} - \tau_o \frac{\tau_R^3}{3} \right] \tag{13}$$

The notation  $\tau_R$  is the wall shear stress and is given by

$$\tau_R = \frac{4Q_z \mu}{\pi R^3} + \frac{4}{3} \tau_o$$

From (9) we have

$$\frac{dp}{dz} = -\frac{2}{R} \tau_R = -\frac{2}{R} \left( \frac{4Q_z \mu}{\pi R^3} + \frac{4}{3} \tau_o \right) \tag{14}$$

This implies that

$$\frac{dp}{dz} = -\frac{8Q_z \mu}{\pi R^4} - \frac{8\tau_o}{3R} \tag{15}$$

Now, suppose  $p = p_\alpha$  when  $z = L_\alpha$  and  $p = p_o$  at  $z = L_o$ , then on integrating (15) above with respect to z yields

$$p_\alpha - p_o = \frac{8Q_z \mu}{\pi R_o^4} \int_0^{L_\alpha} \left( \frac{R}{R_o} \right)^{-4} dz - \frac{8\tau_o}{3R_o} \int_0^{L_\alpha} \left( \frac{R}{R_o} \right)^{-1} dz \quad \alpha \geq 1 \tag{16}$$

Thus, the resistance to flow is the ratio of the pressure difference to the flux  $Q_z$ . Let  $\rho$  represent the resistance to flow, then we have

$$\rho = \frac{p_\alpha - p_o}{Q_z} = \frac{8\mu}{\pi R_o^4} \int_0^{L_\alpha} \left( \frac{R}{R_o} \right)^{-4} dz - \frac{8\tau_o}{3Q_z R_o} \int_0^{L_\alpha} \left( \frac{R}{R_o} \right)^{-1} dz \tag{17}$$

$$= \Gamma_1 \int_0^{L_\alpha} \left( \frac{R}{R_o} \right)^{-4} dz + \Gamma_2 \int_0^{L_\alpha} \left( \frac{R}{R_o} \right)^{-1} dz, \tag{18}$$

where  $\Gamma_1 = -\frac{8\mu}{\pi R_o^4}$  and  $\Gamma_2 = -\frac{8\tau_o}{3Q_z R_o}$

$$\rho = \Gamma_1 \left[ \int_0^{\frac{\gamma}{(n-1)L_o}} \left( \frac{R}{R_o} \right)^{-4} dz + \sum_{n=1}^{n=n \max} \int_{\frac{(n-1)L_o}{\gamma}}^{\frac{nL_o}{\gamma}} \left( \frac{R}{R_o} \right)^{-4} dz + \int_{\frac{nL_o}{\gamma}}^{L_\alpha} \left( \frac{R}{R_o} \right) dz \right] + \Gamma_2 \left[ \int_0^{\frac{\gamma}{(n-1)L_o}} \left( \frac{R}{R_o} \right)^{-1} dz + \sum_{n=1}^{n=n \max} \int_{\frac{(n-1)L_o}{\gamma}}^{\frac{nL_o}{\gamma}} \left( \frac{R}{R_o} \right)^{-1} dz + \int_{\frac{nL_o}{\gamma}}^{L_\alpha} \left( \frac{R}{R_o} \right) dz \right] \tag{19}$$

Taking  $n = 2$  we have the following:

$$\rho = \Gamma_1 \left[ \int_0^{\frac{L_o}{\gamma}} \left( \frac{R}{R_o} \right)^{-4} dz + \int_{\frac{L_o}{\gamma}}^{\frac{2L_o}{\gamma}} \left( \frac{R}{R_o} \right)^{-4} dz + \int_{\frac{2L_o}{\gamma}}^{L_\alpha} \left( \frac{R}{R_o} \right) dz \right] + \Gamma_2 \left[ \int_0^{\frac{L_o}{\gamma}} \left( \frac{R}{R_o} \right)^{-1} dz + \int_{\frac{L_o}{\gamma}}^{\frac{2L_o}{\gamma}} \left( \frac{R}{R_o} \right)^{-1} dz + \int_{\frac{2L_o}{\gamma}}^{L_\alpha} \left( \frac{R}{R_o} \right) dz \right] \tag{20}$$

$$\rho = \Gamma_1 \left[ \frac{L_o}{\gamma} - \frac{2L_o}{\gamma} + L_\alpha \right] + \Gamma_2 \left[ \frac{L_o}{\gamma} - \frac{2L_o}{\gamma} + L_\alpha \right] + (\Gamma_1 I_1 + \Gamma_2 I_2) + (\Gamma_1 J_1 + \Gamma_2 J_2) \tag{21}$$

$$\rho = (\Gamma_1 + \Gamma_2) \left( L_\alpha - \frac{L_o}{\gamma} \right) + (\Gamma_1 I_1 + \Gamma_2 I_2) + (\Gamma_1 J_1 + \Gamma_2 J_2), \tag{22}$$

where  $I_1 = \int_0^{\frac{L_o}{\gamma}} \left( \frac{R}{R_o} \right)^{-4} dz$  and  $J_1 = \int_{\frac{L_o}{\gamma}}^{\frac{2L_o}{\gamma}} \left( \frac{R}{R_o} \right)^{-4} dz$  (23)

$$I_2 = \int_0^{\frac{L_o}{\gamma}} \left( \frac{R}{R_o} \right)^{-1} dz \text{ and } J_2 = \int_{\frac{L_o}{\gamma}}^{\frac{2L_o}{\gamma}} \left( \frac{R}{R_o} \right)^{-1} dz \tag{24}$$

Now in a healthy condition when the stenoses are absent the quantity  $L_o = 0$  and  $I_1 = I_2 = J_1 = J_2 = 0$ .

Therefore substituting in (22) we have

$$\rho_N = (\Gamma_1 + \Gamma_2) L_\alpha \tag{25}$$

Where  $\Gamma_1$  and  $\Gamma_2$  are as defined in (18).

Let  $\zeta = \frac{\rho}{\rho_N} = \frac{(\Gamma_1 + \Gamma_2) \left( L_\alpha - \frac{L_o}{\gamma} \right) + (\Gamma_1 I_1 + \Gamma_2 I_2) + (\Gamma_1 J_1 + \Gamma_2 J_2)}{(\Gamma_1 + \Gamma_2) L_\alpha}$  (26)

$$= 1 - \frac{L_o}{\gamma L_\alpha} + \frac{\Gamma_1 (I_1 + J_1) + \Gamma_2 (I_2 + J_2)}{(\Gamma_1 + \Gamma_2) L_\alpha} \tag{27}$$

The shear stress in the normal condition is given as

$$\tau_N = \frac{4Q_z \mu}{\pi R_o^3} \tag{28}$$

Based on our formulation, the wall stress ratio is given by

$$T_r = \frac{\tau_R}{\tau_N} = \frac{1}{\left( \frac{R}{R_o} \right)^3} + \frac{\pi R_o^3 \tau_o}{3Q_z \mu} \tag{29}$$

At the mid-point of the second stenosis,  $R = R_o - \delta h$ , and

$$T_r = \frac{1}{\left( 1 - \frac{\delta h}{R_o} \right)^3} + \frac{\pi R_o^3 \tau_o}{3\pi Q_z} \tag{30}$$

On taking  $n = 2$ ,  $d = 0$  and  $R = R_o - \delta h$  (1) becomes

$$\frac{R_o - \delta h}{R_o} = 1 - \varepsilon \left[ L_o^{s-1} (\gamma z - L_o) - (\gamma z - L_o)^s \right] \tag{31}$$

Thus, we have

$$1 - \frac{\delta h}{R_o} = 1 - \varepsilon \left[ L_o^{s-1} (\gamma z - L_o) - (\gamma z - L_o)^s \right] \tag{32}$$

$$\frac{\delta h}{R_o} = \varepsilon \left[ L_o^{s-1} (\gamma z - L_o) - (\gamma z - L_o)^s \right] \tag{33}$$

$$\varepsilon = \frac{\delta h}{R_o \left[ L_o^{s-1} (\gamma z - L_o) - (\gamma z - L_o)^s \right]} \tag{34}$$

$\delta h$  is the height of the stenosis at

$$z = \frac{L_o \left( 1 + \frac{1}{s^{1/s-1}} \right)}{\gamma} \tag{35}$$

**IV. Numerical computation and graphical representation**

In this section, results from numerical computations as well as graphical representations are presented. The values from numerical computations used in generating Figures 3-7 are given in the Appendix. Unless otherwise stated, the following values were used for the numerical computations:  $\frac{\delta h}{R_o} = 0 - 0.5$ ,  $\tau_o = 0.03$ ,  $Q_z = 2 \times 10^{-4}$ ,  $\gamma = 1 - 2$ ,  $\mu = 4.03 \times 10^{-2}$ ,  $S = 2 - 15$ ,  $n = 2 - 5$ .

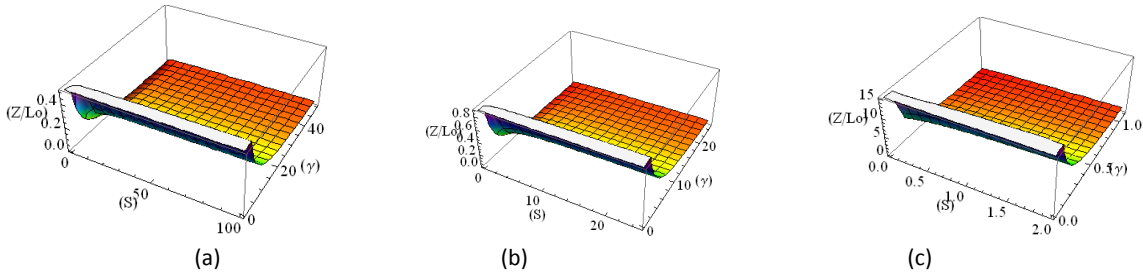


Figure 2: The variation of  $\frac{Z}{L_0}$  with different values of the shape parameter (s) and the positive number  $\gamma \geq 1$

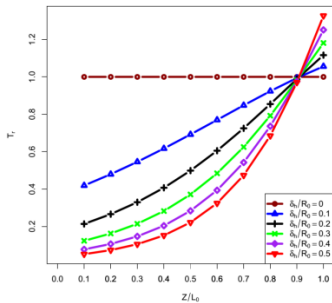


Figure 3: Variation of  $T_r$  with  $\frac{Z}{L_0}$  for different  $\frac{\delta_h}{R_0}$ .  $S = 2, \gamma = 1.1$ .

The variation of wall shear stress  $T_r$  with axial distance  $\frac{Z}{L_0}$  for different fixed values of stenosis height  $\frac{\delta_h}{R_0}$  in the range of values 0 to 0.5 is plotted in Figure 3. The wall shear stress follows similar pattern for various values of stenosis height in the range of  $0 < \frac{\delta_h}{R_0} \leq 1$ . The values of  $T_r$  increases with axial distance  $\frac{Z}{L_0}$ . The magnitude of the increment of  $T_r$  also increases with axial distance. On the other hand, the values of  $T_r$  decreases as stenosis height  $\frac{\delta_h}{R_0}$  increases for fixed values of  $\frac{Z}{L_0}$  ranging from 0.1 to 0.9, but then increases with  $\frac{\delta_h}{R_0}$  for values of  $\frac{Z}{L_0}$  in the range of 0.9 - 1.0.

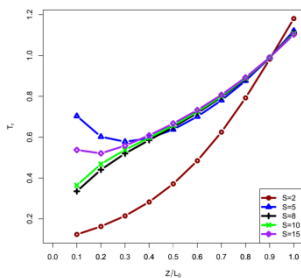


Figure 4: The variation of  $T_r$  with  $\frac{Z}{L_0}$  for different  $S$ .  $\frac{\delta_h}{R_0} = 0.3, \gamma = 1.1$ .

Figure 4 illustrates the variation of wall shear stress  $T_r$  with axial distance  $\frac{Z}{L_0}$  for different stenosis shape parameter  $S$  in the range of values 2 to 15. When the shape parameter takes value  $S = 5$ , the wall shear stress initially decreases as values of the axial distance increases from 0.1 to 0.3 but for values of the axial distance greater than 0.3, the wall shear stress shows increasing pattern. Similarly, when the shape parameter takes value  $S = 15$ , the wall shear stress initially decreases as values of the axial distance increases from 0.1 to 0.2 but shows increasing pattern for values of the axial distance greater than 0.2. For values of  $S = 2, 8, 10$ , the shear stress increases with axial distance.

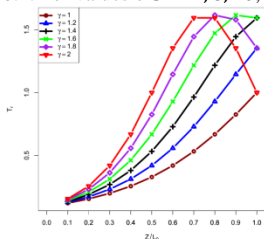


Figure 5: The variation of  $T_r$  with  $\frac{Z}{L_0}$  for different  $\gamma, S = 2, \frac{\delta_h}{R_0} = 0.3$ .

The variation of wall shear stress  $T_r$  with axial distance  $\frac{Z}{L_o}$  for different fixed values of  $\gamma$  in the range of 1 to 2 is illustrated by Figure 5. The plot indicates that  $T_r$  increases as  $\frac{Z}{L_o}$  increases up to certain values and then decreases. Similarly, for fixed values of  $\frac{Z}{L_o}$ , the value of  $T_r$  increases with  $\gamma$  up to a certain value and then decreases.

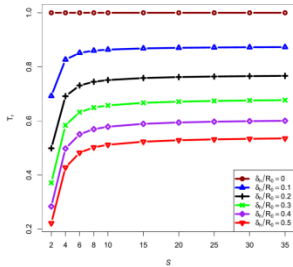


Figure 6: The variation of  $T_r$  with  $S$  for different  $\frac{\delta_h}{R_o} \cdot \frac{Z}{L_o} = 0.5, \gamma = 1.1$ .

Figure 6 presents the variation of wall shear stress  $T_r$  with stenosis shape parameter  $S$  for fixed values of stenosis height  $\frac{\delta_h}{R_o}$  in the range of 0 to 0.5. The plot indicates that for  $\frac{\delta_h}{R_o} = 0$ ,  $T_r$  remains fixed, but for higher values of  $\frac{\delta_h}{R_o}$ ,  $T_r$  increases rapidly for values of  $S$  in the range 2-6 but as  $S$  increases the magnitude of the variation in  $T_r$  drops considerably. Similarly, the values of  $T_r$  increase with  $\frac{\delta_h}{R_o}$  for fixed values of  $\frac{Z}{L_o}$  and  $S$ .

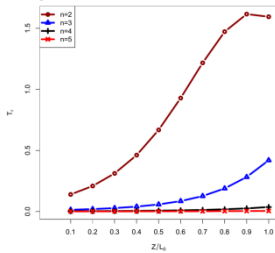


Figure 7: The variation of  $T_r$  with  $\frac{Z}{L_o}$  for different values of  $n, S=2, \frac{\delta_h}{R_o} = 0.3, \gamma = 1.6$ .

Figure 7 illustrates the variation of wall shear stress  $T_r$  with axial distance  $\frac{Z}{L_o}$  for fixed values of  $n$  (number of stenosis in the artery) in the range of values 2 to 5. The plot indicates that the steepness of the variation of  $T_r$  with  $\frac{Z}{L_o}$  decreases as  $n$  increases. When  $n = 2$ ,  $T_r$  increases rapidly for values of  $\frac{Z}{L_o}$  in the range 0.1 - 0.9 but decreases for values of  $\frac{Z}{L_o}$  in the range 0.9 - 1.0. For  $n = 4, 5$ ,  $T_r$  increases very slowly with  $\frac{Z}{L_o}$ . Also,  $T_r$  increases with number of stenosis  $n$  for fixed values of  $\frac{Z}{L_o}$ .

**V. Conclusion**

In the present article, making use of the Bingham plastic model of blood flow, we are able to obtain an analytic relation for the resistance to flow for a chronic, multiple and overlapped stenosed artery. We assume a negligible distance between the stenosis and consider its effect on the flow resistance. The effect of an increase in the height of the stenosis was also investigated, as well as the effect of growth in the parameter  $\gamma$ , even though it culminates to insignificant variation for different values of the stenosis height.

The results in this article may provide a physician with supplementary information for the diagnosis and treatment of this fatal disease.

**Appendix: Tables of Values from Numerical Computations**

Table 1: Variation of  $T_r$  with  $\frac{Z}{L_o}$  for different  $\frac{\delta_h}{R_o}, S = 2, \gamma = 1.1$ .

$\frac{Z}{L_o} \downarrow$	$\frac{\delta_h}{R_o} \rightarrow$					
	0	0.1	0.2	0.3	0.4	0.5
0.1	1.000167	0.419126	0.213785	0.123447	0.077648	0.051996
0.2	1.000167	0.479607	0.265938	0.162529	0.106510	0.073564
0.3	1.000167	0.545787	0.329845	0.214360	0.147090	0.105283
0.4	1.000167	0.617042	0.407115	0.282595	0.204112	0.152211
0.5	1.000167	0.692298	0.498885	0.371318	0.283800	0.221770
0.6	1.000167	0.769975	0.605345	0.484503	0.393806	0.324413
0.7	1.000167	0.847966	0.725149	0.624954	0.542403	0.473778
0.8	1.000167	0.923676	0.854791	0.792590	0.736281	0.685184
0.9	1.000167	0.994132	0.988144	0.982205	0.976314	0.970469
1	1.000167	1.056171	1.116436	1.181376	1.251452	1.327182

Table 2: The variation of  $T_r$  with  $\frac{Z}{L_0}$  for different  $S, \frac{\delta_h}{R_0} = 0.3, \gamma = 1.1$ .

$\frac{Z}{L_0} \downarrow$	$S \rightarrow$				
	2	5	8	10	15
0.1	0.123447	0.703722	0.334987	0.364126	0.537415
0.2	0.162529	0.602298	0.440533	0.468408	0.520893
0.3	0.214360	0.577974	0.520067	0.538326	0.558299
0.4	0.282595	0.594560	0.585701	0.597071	0.608881
0.5	0.371318	0.637802	0.649413	0.657489	0.666962
0.6	0.484503	0.701010	0.718406	0.724797	0.732772
0.7	0.624954	0.780896	0.796519	0.801395	0.807539
0.8	0.792590	0.876487	0.886239	0.889163	0.892837
0.9	0.982205	0.989001	0.989952	0.990233	0.990586
1	1.181376	1.121650	1.110502	1.107224	1.103144

Table3: The variation of  $T_r$  with  $\frac{Z}{L_0}$  for different  $\gamma, S = 2, \frac{\delta_h}{R_0} = 0.3$ .

$\frac{Z}{L_0} \downarrow$	$\gamma \rightarrow$					
	1	1.2	1.4	1.6	1.8	2
0.1	0.120416	0.126557	0.133026	0.139840	0.147016	0.154572
0.2	0.154572	0.170905	0.189000	0.209029	0.231176	0.255632
0.3	0.198762	0.231176	0.268788	0.312268	0.362297	0.419521
0.4	0.255632	0.312268	0.380542	0.461951	0.557646	0.668083
0.5	0.328184	0.419521	0.532342	0.668083	0.825689	1.000167
0.6	0.419521	0.557646	0.728677	0.928875	1.145270	1.353781
0.7	0.532342	0.728677	0.964328	1.217143	1.445002	1.594499
0.8	0.668083	0.928875	1.217143	1.472392	1.616149	1.594499
0.9	0.825689	1.14527	1.445002	1.616149	1.579838	1.353781
1	1.000167	1.353781	1.594499	1.594499	1.353781	1.000167

Table 4: The variation of  $T_r$  with  $S$  for different  $\frac{\delta_h}{R_0}, \frac{Z}{L_0} = 0.5, \gamma = 1.1$ .

$S \downarrow$	$\frac{\delta_h}{R_0} \rightarrow$					
	0	0.1	0.2	0.3	0.4	0.5
2	1.000167	0.692298	0.498885	0.371318	0.2838	0.22177
4	1.000167	0.826927	0.691500	0.584107	0.497854	0.427785
6	1.000167	0.851789	0.731373	0.632629	0.550893	0.482656
8	1.000167	0.860017	0.744879	0.649413	0.569592	0.502337
10	1.000167	0.863911	0.751327	0.657489	0.578652	0.511935
15	1.000167	0.868429	0.758850	0.666962	0.589333	0.523301
20	1.000167	0.870532	0.762370	0.671413	0.594371	0.528682
25	1.000167	0.871764	0.764435	0.674030	0.597339	0.531857
30	1.000167	0.872572	0.765792	0.675752	0.599294	0.533951
35	1.000167	0.873143	0.766752	0.676970	0.600679	0.535436

Table 5: The variation of  $T_r$  with  $\frac{Z}{L_0}$  for different  $n, S=2, \frac{\delta_h}{R_0} = 0.3, \gamma = 1.6$ .

$\frac{Z}{L_0} \downarrow$	$n \rightarrow$			
	2	3	4	5
0.1	0.13984	0.014307	0.002497	0.000724
0.2	0.209029	0.019886	0.003188	0.000854
0.3	0.312268	0.028038	0.004124	0.001020
0.4	0.461951	0.040096	0.005406	0.001233
0.5	0.668083	0.058126	0.007182	0.001510
0.6	0.928875	0.085325	0.009671	0.001873
0.7	1.217143	0.126557	0.013206	0.002354
0.8	1.472392	0.189000	0.018290	0.002996
0.9	1.616149	0.282595	0.025696	0.003862
	1.594499	0.419521	0.036618	0.005046

References

- [1] Ahmed, S. Bingham Plastic Fluid Model for Steady Flow of Blood with Velocity Slip Tube Wall in Presence of Magnetic Field. Asian Journal of Technology & Management Research, 2015. Vol.5:1. P. 57-70. ISSN: 2249-0892
- [2] Yadav, S. S. and Kumar, K. Bingham Plastic Characteristics of Blood Flow Through a Generalized Atherosclerotic Artery with Multiple Stenoses. Advances in Applied Science Research, 2012. Vol. 3:6. P. 3551-3557. ISSN: 0976-8610

- [3] Singh, A.K and Singh, D. P. A Computational Study of Bingham Plastic Flow of Blood Through an Artery by Multiple Stenoses and Post Dilation. *Advances in Applied Science Research*, 2012. Vol. 3:5.P. 3285-3290.ISSN: 0976-8610
- [4] Verma, S. R. Mathematical Modeling of Bingham Plastic Model of Blood Flow Through Stenotic Vessel. *International Journal of Engineering Research and Applications*, 2014. Vol. 4:12. P. 11-17.
- [5] Nanda,S.,Basu, M. B., Das, S.,Sundar,C. S., Ghosh, S and Bhattacharya, S. A Study on Bingham Plastic Characteristics of Blood Flow Through Multiple Overlapped Stenosed Arteries. *Saudi Journal of Engineering and Technology*, 2017.Vol.2:9. P. 349-357.
- [6] Venkatesan J., Sankar D. S., Hemalatha K., Yatim Y. Mathematical Analysis of Casson Fluid Model for Blood Rheology in Stenosed Narrow Arteries. *Journal of Applied Mathematics*. 2013;2013doi: 10.1155/2013/583809.583809
- [7] V.P Sirivestava, V.Rochana, M. Shailesh, and S. Poonam.A Two Layer Non-Newtonian Blood Flow Through an Overlapping Constriction. *Applications and Applied Mathematics: An International Journal*, 2011. Vol6.P. 1781-1797
- [8] Oghre, E.O. and Okoronkwo F.M. Bingham Fluid Model for Steady Flow in a Multi-Irregular Stenosed Artery. *Transactions of the Nigerian Association of Mathematical Physics* 2016.Vol2.P. 291-298.